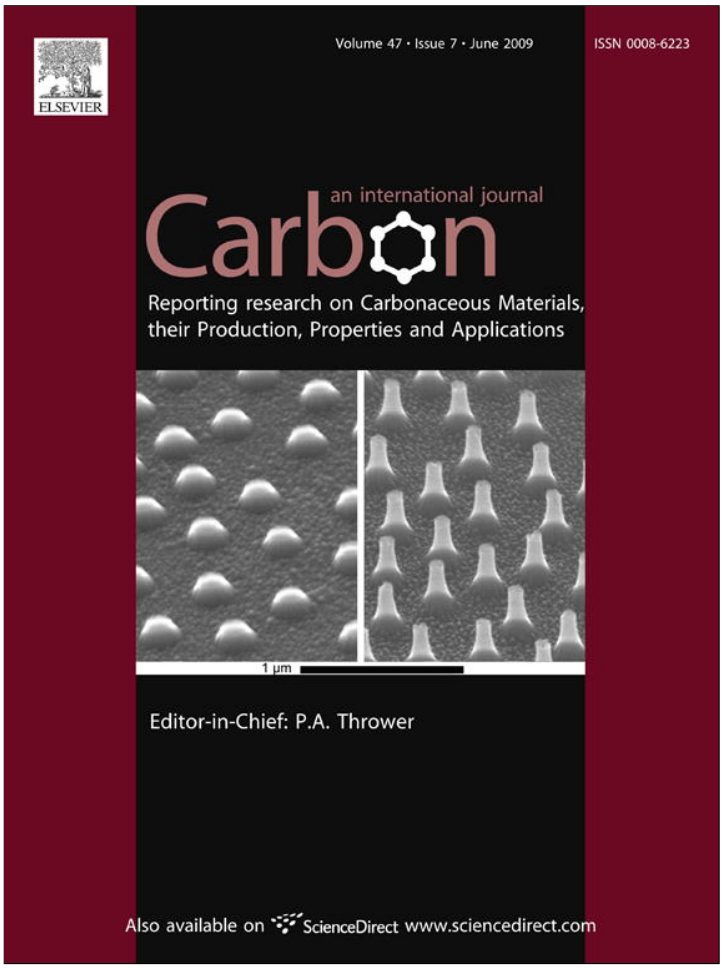

CARBON 47 (2009) 1841–1845

available at www.sciencedirect.com

ScienceDirect

journal homepage: www.elsevier.com/locate/carbon

The characterization and application of p-type semiconducting mesoporous carbon nanofibers

Lei Liao[a,b], *Mingbo Zheng*[c], *Zhou Zhang*[a], *Bin Yan*[a], *Xiaofeng Chang*[c], *Guangbin Ji*[c], *Zexiang Shen*[a], *Tom Wu*[a], *Jieming Cao*[c], *Jixuan Zhang*[d], *Hao Gong*[d], *Jian Cao*[c], *Ting Yu*[a,*]

[a]*Division of Physics and Applied Physics, School of Physical and Mathematical Sciences, Nanyang Technological University, Singapore 637371, Singapore*

[b]*Department of Physics, Wuhan University, Wuhan, 430072, China*

[c]*Nanomaterials Research Institute, College of Materials Science and Technology, Nanjing University of Aeronautics and Astronautics, Nanjing 210016, China*

[d]*Department of Materials Science and Engineering, National University of Singapore, 117576, Singapore*

ARTICLE INFO

Article history:
Received 23 November 2008
Accepted 9 March 2009
Available online 16 March 2009

ABSTRACT

The microstructures of mesoporous carbon nanofibers were characterized by scanning electron microscopy, transmission electron microscopy, nano-Raman, nitrogen adsorption–desorption and optical transmission. They possessed a high specific surface area 840 $m^2 g^{-1}$ and a 1.07 eV band gap. All mesoporous carbon nanofiber network can act as the channel material in p-type field-effect transistor devices with field-effect mobilities over 10 cm^2/V s. Furthermore, mesoporous carbon nanofiber network exhibits better sensitivity and faster response to NO_2 gas than that of carbon nanotubes, which makes it a promising candidate as poisonous gas sensing nanodevices.

1. Introduction

Carbon nanomaterials have been the focus of nanoscience and nanotechnology because of their practical applications as building blocks of nanoscaled optoelectronics, electronics, and chemical/biosensing devices during the past decades [1,2]. In particular, carbon nanotubes (CNTs) and nanofibers, have attracted much attention in both academic and industrial research. Applications as field emitters, electromagnetic wave absorbers or filters, nanosensors have been demonstrated in laboratorial devices [3–5].

Comparing to other members in carbon nanomaterial family, mesoporous carbon nanofibers are characterized with higher specific surface area and better gas permeability. These unique features may provide them with potential applications in gas sensor, electrode materials, catalysis, hydrogen storage, adsorption and other fields. Up to date, however, most of the efforts have been devoted to the growth of mesoporous carbon nanofibers. For example, mesoporous carbon nano-filaments were fabricated from the replication of silica-based mesoporous nano-filaments prepared in the channels of anodic alumina membranes (AAO) [6]. Besides, nanoporous carbon nanotubes were synthesized using AAO as template [7]. There were few reports on the application of such materials with respect to their advantages.

We previously reported the synthesis of mesoporous carbon nanofibers (MCNFs) within the pores of AAO through an easy one-step template method. In this paper, the structure of MCNFs is characterized carefully, and the applications of mesoporous carbon nanofiber network as field-effect transistor (FET) and gas sensor are reported. In contrast to CNTs, whose metallic or semiconducting behaviors are difficult to be controlled, all MCNFs network FETs exhibit p-type semiconducting behaviors with the band gap of about 1.07 eV, a

* Corresponding author:
E-mail address: yuting@ntu.edu.sg (T. Yu).
0008-6223/$ - see front matter
doi:10.1016/j.carbon.2009.03.029

promising and critical property for future carbon-based electronics. Furthermore, the MCNFs network exhibits good sensitivity and fast response to NO_2 gas because of their large surface area and semiconducting behavior, which makes it a promising candidate as poisonous gas sensing nanodevices.

2. Experimental

The MCNFs were synthesized by the method reported in our previous work [8]. The Pluronic F127/resol mixture ethanol solution of FDU-16 was used as the precursor solution [9]. An AAO template with an average pore size of about 60 nm was added into the solution. The solution was dried at room temperature. The sample was then taken out and heated at 100 °C for 24 h to thermopolymerize the phenolic resins, followed by heating at 700 °C in nitrogen for 3 h to carbonize. MCNFs were obtained by dissolving the AAO template in 10% aqueous HF adsorption–desorption analysis.

Transmission electron microscopy (TEM) imaging and electron energy loss spectroscopy (EELS) measurements were performed on a 200 kV JEOL 2010F field-emission-gun TEM equipped with a Gatan electron energy loss spectrometer. For scanning electron microscopy (SEM) characterization, the mesoporous carbon nanofibers (MCNFs) were placed on the conductive tape for direct observation with a JEOL 6700 microscope, operated at 10 kV. The Raman spectra were carried out with a WITEC CRM200 confocal Raman system. The spot size is about 300 nm and the excitation power density 2×10^3 W/cm^2. A wideband invisible laser (KOHERAS) serves as the input light to investigate the absorption spectrum of CNF. Such laser could range from 700 nm to 1700 nm. Firstly, we measure the input spectra directly with an optical spectrum analyzer (Ando AQ-6315B). We drop the solution of CNF at the pinhole of our fiber pigtail and then let the input laser pass through the sample. The output spectrum would be recorded as well. The absorption spectra of our CNF can be considered to be the difference between the input and output spectra.

The electrical transport properties were measured by Cascade probe station with Agilent 4157B and Suss probe station with Keithley 4200 SCS. Finally, after wire-bonding to a supporting chip, gas sensing properties of the devices were examined at room temperature. The nitrogen adsorption–desorption isotherms at 77 K were measured using an ASAP 2010 analyzer (Micromeritics Co. Ltd.). The testing gases employed in this work were pure air and 5–40 ppm test gases in air. The gas sensitivity of the devices was defined as the ratio of the electrical resistance in testing gases (R_g) to that in air (R_a).

3. Results and discussion

A low-magnification SEM image (Fig. 1a) shows that the aligned MCNFs on are about 80 microns in length, and about

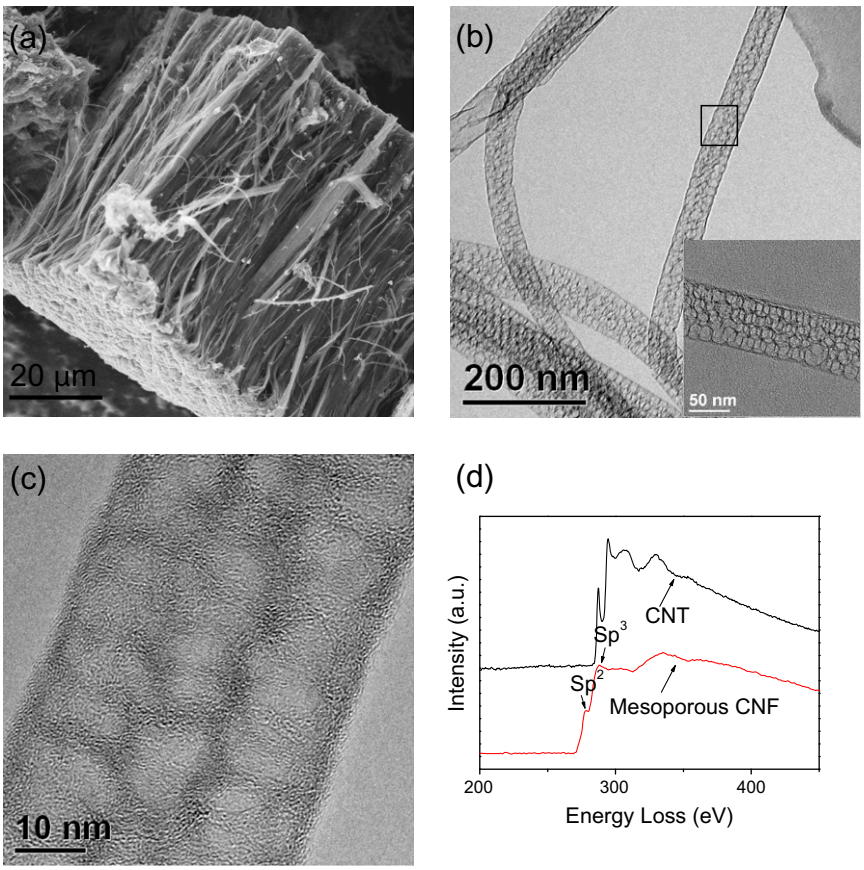

Fig. 1 – (a) SEM image of MCNFs. (b) Low magnification TEM image of MCNFs. Inset shows a single MCNF. (c) HRTEM image of MCNF taken from the square section in Fig. 1b. (d) EELS spectra taken on CNT and MCNF.

50–100 nm in diameter. The mesoporous structure was characterized by transmission electron microscopy, which showed many mesopores on MCNFs with an average pore diameter of 15 nm (Fig. 1b). The inset of Fig. 1b clearly shows a single MCNF. No graphitic lattice was observed in the high-resolution TEM (HRTEM) image (Fig. 1c), which suggests that MCNF is amorphous. Fig. 1d shows EELS spectra taken from CNT and MCNF. In the EELS spectrum of the commercial CNT, *k*-edges of *C* can be clearly identified. A peak at 285 eV is due to the excitation to $p\pi^*$ states of sp^2, and a step at 290 eV results from the excitation to $p\sigma^*$ states of sp^3 and sp^2.[6] Meanwhile, the EELS of MCNF exhibits the amorphous characteristics because of the degradation of the $p\pi^*$ state [10].

Fig. 2a shows the Raman spectrum of the MCNFs. G band at 1596 cm^{-1}, is actually the stretching vibration of any pair of sp^2 sites, whether in C=C chains or in aromatic rings, was recorded for our MCNFs. The appearance of D band at 1350 cm^{-1} indicates a high degree of disorder in the MCNFs [10]. The micro-Raman mappings of a MCNFs network nanodevice are shown in Fig. 2b. From the G band and D band mapping, the numbers of MCNFs between source and drain could be obtained easily and it is a non-contact method. Fig. 2c shows optical transmission loss spectrum of MCNFs, which exhibits an obvious adsorption at 1150 nm. The result reveals that the MCNFs are semiconducting and the band gap is about 1.07 eV. Fig. 2d shows the nitrogen gas adsorption–desorption isotherms for the samples. The pore size distribution from the adsorption branches is shown in inset of Fig. 2d, which was consistent with the results of TEM. It is noticeable that MCNFs has a small distribution in the range of 10–20 nm. The surface area of MCNFs is 840 $m^2\ g^{-1}$, which is larger than that of commercial carbon nanotubes.

A schematic device diagram of MCNFs network is shown in Fig. 3a. The temperature-dependent transport property was studied (see Fig. 3b). From 300 to 460 K, the resistivity of MCNFs decreases with increasing temperature, which exhibits its semiconductors behavior. Fig. 3c displays the I_{ds}–V_{ds} curves of a typical MCNFs network FET. From the I_{ds}–V_{ds} curves obtained under gate voltages (V_g) of −30, −20, −10, 0, and 10 V, it can be clearly seen that the conductance of the nanofiber decreases monotonically as the gate potential increases, indicating that the MCNF FET is a typical p-channel FET. Inset of Fig. 3c shows the I_{ds}–V_g curves of the MCNFs network FET. The carrier concentration is estimated to be $n = 4.6 \times 10^8\ cm^{-1}$, which corresponds to a bulk concentration of $1.5 \times 10^{18}\ cm^{-3}$, and the mobility is calculated to be $\mu = 10\ cm^2/V\ s$ at $V_g = 0$ V [11]. The band gap (about 1.07 eV) of the MCNFs was obtained by optical transmission loss spectrum, which is discussed by considering the cluster model [10]. The sp^2 sites have a variable gap, which depends on the configuration of each sp^2 cluster. Because that the sp^3 sites have a wider gap with respect to the sp^2 sites, between the σ and σ^* states, the sp^3 matrix acts as a tunnel barrier between the sp^2 clusters. The inhomogeneous and random distribution of sp^2 gaps creates disorder, and therefore, the band gap of amorphous carbon is an average of the band gaps of the embedded clusters. In fact, most of the amorphous carbon films have been proved to be weak p-type semiconductors [10]. Since the MCNFs consist of an inhomogeneous mixture of sp^2 and sp^3 sites as suggested by the EELS results

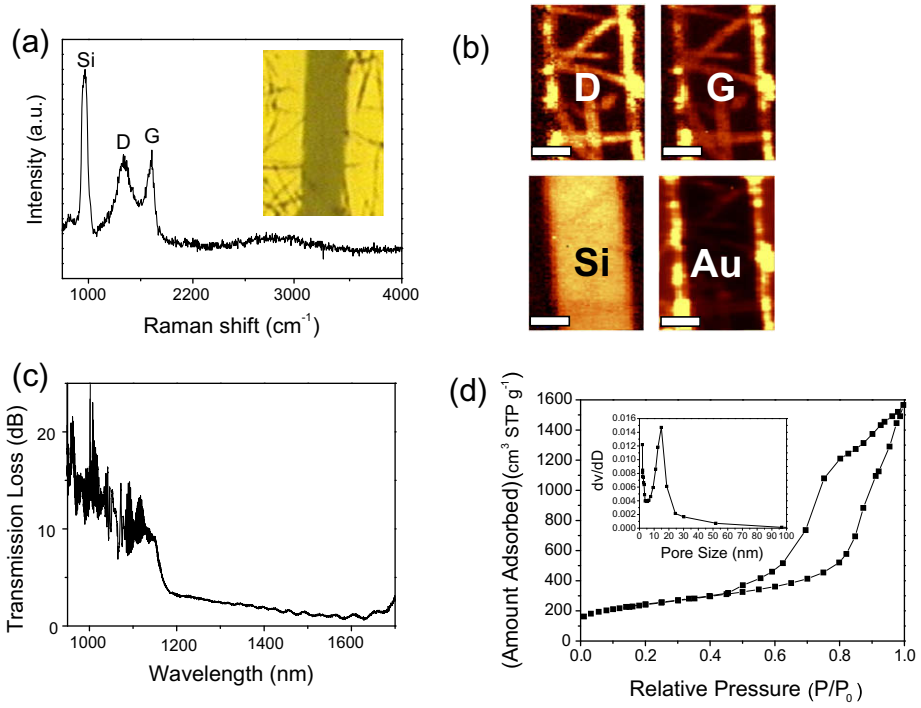

Fig. 2 – (a) Raman spectrum of MCNFs, inset image shows the optical image of the nanodevice. (b) Raman mapping of the nanodevices by extracting the integrated intensities of D band, G band of carbon and Si mode, Au fluorescence mapping, scale bar = 1 μm. (c) The optical transmission spectra of MCNFs. (d) Nitrogen adsorption–desorption isotherms and pore size distribution plots of the samples.

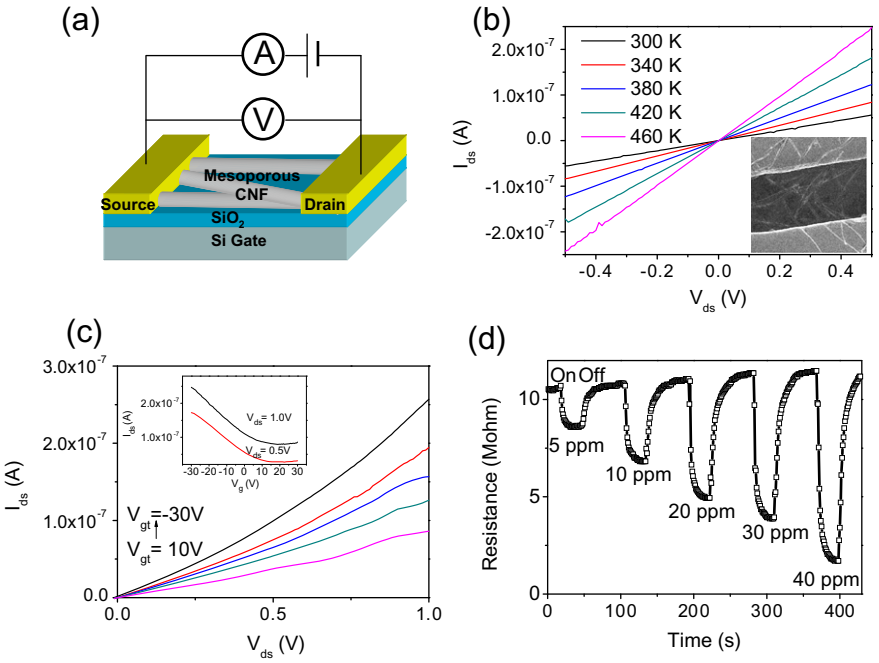

Fig. 3 – (a) The diagram of configuration of a MCNFs network field-effect transistor. (b) Temperature-dependent *I–V* curves of MCNFs network device, inset shows SEM image of a MCNFs network FET, scale bar = 1 μm. (c) I_{ds}–V_{ds} curves of a MCNFs network FET. Inset shows I_{ds}–V_{gt} curves of a MCNFs network FET. (d) The gas sensibility response of a MCNFs network for different NO_2 concentrations.

in Fig. 1d, it is reasonable that the MCNFs in our case are weak semiconductors [10].

In late years, interests in the air pollutants and its monitoring have been growing in our life. Nitrogen oxides like nitrogen monoxide (NO) and nitrogen dioxide (NO_2) are typical air pollutants that cause environmental problems. There are demands for a small and cheap gas sensor for NO detection in medical field and its basic research area. From this point of view, it is necessary to develop high sensitive and inexpensive NO_x gas sensors to detect low concentrate NO and NO_2 gases. CNTs are expected as a new gas sensing material, which has an outstanding high sensitivity at a low temperature with a fast response. Many gas sensors based on either multi-walled or single-walled CNTs have been reported [12–14]. Herein, we fabricated gas sensors based on MCNFs networks. The gas sensing properties of the devices were examined at room temperature. The testing gases employed in this work were pure air and 5–40 ppm test gases in air. Interestingly, we found that they have a high sensitivity to NO_2. Fig. 3d is the *R–t* (Resistance vs. time) curve of a MCNFs network gas sensor subjected to NO_2 with various concentrations. It can be seen that the MCNFs network sensor has a good sensing performance, with a high NO_2 sensitivity (about 5 ppm) and a short response time (less than 10 s). Similar results were obtained on another ten devices. The performance of the gas sensor based on MCNFs is better than that of CNT gas sensor [15,16], which may be contributed to their large surface area and p-type semiconducting behavior. During gas sensing, the electronic properties of the MCNFs are altered by a direct charge transfer between the gas and the nanofiber surface. The electron-donor gas and electron-acceptor gas induces opposite effect on the electrical transport of a p-type semiconductor. As a consequence, electrons are transferred to NO_2 (electron-acceptor gas) molecules from the valence band of the MCNFs, increasing the density of holes, thereby decreasing the electrical resistance [16].

Moreover, the sensing mechanism in carbon nanomaterials has been widely investigated by theoretical ab-initio calculations. Ab-initio calculations on a semiconducting (10,0) CNT predict physisorption with adsorption energies between 0.3 and 0.8 eV that leads to an increase in the p-type channel conductance due to electron transfer of 0.1e per NO_2 molecule from the SWNT to NO_2. These calculations, however, also predict a desorption from the SWNT of the NO_2 molecules within tenths of seconds [17]. NO_2 molecules are weakly adsorbed on carbon nanomaterials with small charge transfer, while they can be either a charge donor or an accepter of the nanotube. The adsorption of some gas molecules on carbon nanomaterials can cause a significant change in electronic and transport properties of the carbon nanomaterials due to the charge transfer and charge fluctuation [18].

Though the gas sensor based on mesoporous carbon nanofiber shows good sensitivity and fast response to NO_2 gas, however, it is not stable for a long run time and short of relative selectivity. It will be burnt up under several μA in a few minutes. In future work, we will go on researching the materials and solving the problems for application.

4. Conclusions

We have characterized the temperature-dependent transport properties of FET devices based on mesoporous carbon nano-

fiber networks. FET devices exhibited p-type semiconducting behavior with field-effect mobility over 10 cm^2/V s at $V_g = 0$ V. Furthermore, the MCNFs network exhibits good sensitivity and fast response to NO_2 gas, which makes it a promising candidate as a sensing unit of poisonous gas sensing nanodevices.

Acknowledgements

Liao L. acknowledges support in this work by the Singapore Millennium Foundation 2008 fellowship. This work was supported by the NSFC (No. 50701024) and Doctor Innovation Funds of Jiangsu Province (BCXJ06-13).

REFERENCES

[1] Iijima S. Helical microtubules of graphitic carbon. Nature 1991;354(6348):56–8.
[2] Novoselov KS, Geim AK, Morozov SV, Jiang D, Zhang Y, Dubonos SV, et al. Electric field effect in atomically thin carbon film. Science 2004;306(5296):666–9.
[3] Che RC, Peng LM, Duan XF, Chen Q, Liang XL. Microwave absorption enhancement and complex permittivity and permeability of Fe encapsulated within carbon nanotubes. Adv Mater 2004;16(5):401.
[4] Tans SJ, Verchueren ARM, Dekker C. Room-temperature transistor based on a single carbon nanotube. Nature 1998;393(6680):49–52.
[5] Zhu YW, Cheong FC, Yu T, Xu XJ, Lim CT, Thong JTL, et al. Effects of CF4 plasma on the field emission properties of aligned multi-wall carbon nanotube films. Carbon 2005;43(2):395–400.
[6] Cott DJ, Petkov N, Morris MA, Platschek B, Bein T, Holmes JD. Preparation of oriented mesoporous carbon nano-filaments within the pores of anodic alumina membranes. J Am Chem Soc 2006;128(12):3920–1.
[7] Bodriguez AT, Chen M, Chen Z, Brinker CJ, Fan H. Nanoporous carbon nanotubes synthesized through confined hydrogen-bonding self-assembly. J Am Chem Soc 2006;128(29):9276–7.
[8] Zheng MB, Cao JM, Ke XF, Ji GB, Chen YP, Shen K, et al. One-step-synthesis of new mesoporous carbon nanofibers through an easy template method. Carbon 2007;45(5):1111–3.
[9] Meng Y, Gu D, Zhang FQ, Shi YF, Yang HF, Li Z, et al. Ordered mesoporous polymers and homologous carbon frameworks: amphiphilic surfactant templating and direct transformation. Angew Chem Int Ed 2005;44(43):7053–9.
[10] Robertson J. Diamond-like amorphous carbon. Mater Sci Eng R 2002;37(4–6):129–281.
[11] Lee YC, Chueh YL, Hsieh CH, Chang MT, Chou LJ, Wang ZL, et al. p-Type alpha-Fe_2O_3 nanowires and their n-type transition in a reductive ambient. Small 2007;3(8):1356–61.
[12] Kong J, Franklin NR, Zhou CW, Chapline MG, Peng S, Cho KJ, et al. Nanotube molecular wires as chemical sensors. Science 2000;287(5453):622–5.
[13] Boussaad S, Diner BA, Fan J. Influence of redox molecules on the electronic conductance of single-walled carbon nanotube field-effect transistors: application to chemical and biological sensing. J Am Chem Soc 2008;130(12):3780–7.
[14] Li J, Lu YJ, Ye Q, Cinke M, Han J, Meyyappan M. Carbon nanotube sensors for gas and organic vapor detection. Nano Lett 2003;3(7):929–33.
[15] Cho WS, Moon S, Paek KK, Lee YH, Park JH, Ju BK. Patterned multiwall carbon nanotube films as materials of NO_2 gas sensors. Sensor Actuator B 2006;119(1):180–5.
[16] Valentini L, Armentano I, Kenny JM, Cantalini C, Lozzi L, Santucci S. Sensors for sub-ppm NO_2 gas detection based on carbon nanotube thin films. Appl Phys Lett 2003;82(6):961–3.
[17] Peng S, Cho KJ, Qi PF, Dai HJ. Ab initio study of CNT NO_2 gas sensor. Chem Phys Lett 2004;387(4–6):271–6.
[18] Zhao JJ, Buldum A, Han J, Lu JP. Gas molecule adsorption in carbon nanotubes and nanotube bundles. Nanotechnology 2002;13(2):195–200.